J Supercomput (2008) 43: 59–76
DOI 10.1007/s11227-007-0138-0

High performance power control and opportunistic fair scheduling in TH-PPM UWB ad-hoc multimedia networks

Yang Liu · Yu-Kwong Kwok · J. Wang

Published online: 1 June 2007

Abstract Ultra wideband (UWB) systems are currently an important wireless infrastructure for high performance short-range communications and mobile applications. Indeed, forming *ad-hoc* networks among various UWB enabled devices is considered as an important mobile data exchange operating environment. In our study, we explore the problem of jointly optimizing the power level and data rate used in the devices in such a UWB based ad-hoc network. We propose a practical optimization algorithm based on judicious power control for real-time applications and opportunistic scheduling for non-real-time applications. Simulation results indicate that our proposed techniques are effective under various practical scenarios.

Keywords High performance wireless networking · Optimal power control · Opportunistic scheduling · TH-PPM UWB · Multimedia · Ad-hoc networks · Proportional fairness

1 Introduction

We consider a joint power and data rate optimization strategy for ultra wideband (UWB) [10, 13, 21] ad-hoc multimedia networks with the coexistence of real-time

A preliminary version of portions of this paper appeared in the *Proceedings of the 7th IEEE Wireless Communications and Networking Conference (WCNC'2006)*, Las Vegas, Nevada, USA, April 2006.

Y. Liu · Y.-K. Kwok (✉)
Department of Electrical and Electronic Engineering, The University of Hong Kong, Pokfulam, Hong Kong
e-mail: ykwok@hku.hk

J. Wang
Department of Electronics, University of Kent, Canterbury CT2 7NT, Kent, UK

(RT) and non-real-time (NRT) applications. As a wideband high performance wireless networking technology, UWB is uniquely characterized by its giga-Hertz transmission bandwidth. Specifically, a UWB signal has a bandwidth over central frequency ratio more than one to fourth. Thus, the spread energy becomes very tiny (only about a few μW per MHz), even lower than the noise level in the normal surroundings. Accordingly, the signal is very short in time (limited in one nanosecond), commonly called *impulse radio*. The use of the impulse radio makes the system multi-path robust, well covert, and can support a high data rate. The different time shifts in the position of one pulse are commonly used to represent the data symbols 0 and 1 in a UWB based communication environment [22]. To eliminate the catastrophic collisions in the multiple access control process, each UWB link uses a distinct pulse-shift pattern called a *time hopping* (TH) code. These TH codes are pseudorandom in order to reduce the interference caused by the other users.

Furthermore, ad-hoc networking is getting popular in wireless communication environments due to its robust self-organizing features [20]. Indeed, an ad-hoc network could work without setting any base station or access point in advance. Because the UWB systems are simple in structure and can provide high rates, ad-hoc over UWB is considered an attractive combination for the high performance wireless personal area networks (WPANs) [8]. These applications can be broadly classified into two types: real-time (RT) and non-real-time (NRT) applications. For example, at home, multimedia devices could easily set up a high speed ad hoc network. Indeed, without any wire-line, the DVD player can be connected to the HDTV, and similarly, photos can be simultaneously downloaded quickly from a digital camera for displaying on a PC in another room.

In UWB ad-hoc networks, scheduling is the process to decide which node(s) should transmit, and power control is used to allocate the power of transmission to corresponding node(s). Several techniques have been reported in the literature about the design of optimization rules and the design of sub-optimal algorithms [4, 17, 19] for scheduling [2, 4, 16, 18] and power control. For instance, the technique suggested in [4] focuses on the scheduling process when a new user gets access and considers the fairness for getting access in UWB ad-hoc networks. On the other hand, a similar method is proposed in [19] and is evaluated with a large number of simulation test cases. One of the findings, which is in accordance with the results reported in [4], is that a node should transmit at peak power or keep silent to achieve the maximum throughput in a UWB network which contains only NRT nodes. In [17], max-min fairness scheduling and power control problems are jointly addressed by a dual approach. Unfortunately, the scenarios considered in all these previous researches are homogeneous—purely RT or purely NRT. Indeed, none of the previous research efforts is for optimizing the system performance in a multimedia application environment, where both RT and NRT applications coexist. Furthermore, it is still considered difficult to satisfy the different fairness requirements (e.g., proportional fairness [11]) in the scheduling of the admitted NRT user. Since RT and NRT nodes always coexist in a practical application scenario, it is worthy exploring further how such a multimedia ad-hoc system shall adjust the RT power and the NRT transmission rate to achieve a comprehensive optimization.

In our study, a practical optimization method is proposed. Specifically, our algorithm maximizes the system throughput while meeting the fairness requirement

Fig. 1 Piconet structure

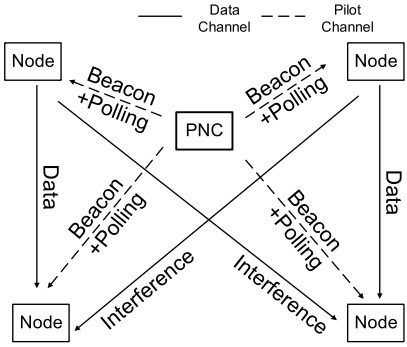

for NRT nodes, and minimizes the power level of RT nodes. Most importantly, the QOS (quality of service) for both types of applications are guaranteed. Furthermore, two suboptimal designs based on the optimized algorithm for large scale systems are studied.

This paper is organized as follows. In Sect. 2, the UWB ad-hoc network system model is presented. The joint optimization strategy when the RT and NRT nodes co-exist is illustrated in Sect. 3. For the RT nodes, power control is the major component since the associated scheduling mechanism is quite simple. On the contrary, for the NRT nodes, meeting the different fairness requirements is the crucial issue. Section 4 reports the optimization results. Finally, Sect. 5 concludes this paper.

2 System model

UWB is expected to supply short-range high data rate service with a small number of users. In our study, we consider a system with a single *piconet*, in which all the nodes are able to communicate with each other directly.

A typical piconet is shown in Fig. 1. Each node in the piconet owns one transmitter and one receiver.

A piconet controller (PNC) is designated to handle the association of new nodes (here, association is the process of admitting one single node into the system), and disassociation of old nodes. Moreover, PNC is in charge of channel access in that it distributes TH code to any newly associated node which has data to transmit. As in the models used in the previous studies, the first node which sets up the piconet is designated as the default PNC. A specified TH code is then chosen by the PNC and used as the pilot channel. Other TH codes are distributed to the transmitter nodes by the PNC as the data channels. As all the nodes are limited in a home-like area, and therefore, can communicate with each other directly, no routing is needed.

Considering the UWB signal's attenuation, we can denote the signal-to-interference-and-noise-ratio (SINR) at the ith link's receiver in a given time slot as follows [4, 22]:

$$\mathrm{SINR}_i = \frac{P_i g_{ii}}{R_i \left(\eta_i + T_f \sigma^2 \sum_{k=1,k\neq i}^{I} P_k g_{ki}\right)}, \quad i = 1, \ldots, I \tag{1}$$

here I is the total number of nodes in the system; P_i is the average power level of the ith link; R_i is the average binary bit rate of the ith link; g_{ij} is the corresponding path gain from the ith link's transmitter to the jth link's receiver; η_i is the background noise; T_f is the time space between two consecutive UWB pulses of one user, i.e., frame time; σ is an inter-user interference parameter depending on the shape of the mono-cycle.

As the interference caused by other nodes is governed by the users' power levels and data rates, we can design an algorithm to determine the optimized values of these two system parameters when the node distribution is known.

3 Joint optimization algorithm

In this section, the joint power control and scheduling algorithm is presented. This algorithm is executed at the beginning of each time slot to manage the wireless channel resources. The design of our proposed algorithm is based on exploiting the specific features of RT and NRT applications.

For the RT applications, each node is required to transmit at every slot, which already defines the scheduling. By contrast, for the NRT applications, power control can be designed according to the following proposition:

Proposition 1 *In the optimal power allocation for a UWB ad-hoc multimedia network, each NRT node in a given time slot either sends at the maximum power or does not send at all.*

Proof This result is derived from the study of the data rate sum projection in any NRT power dimension. The findings in [19] and [4] reveal that each node should either send with the peak power or keep silent to maximize the system throughput when there are only NRT nodes in the system. That is, the projection of the throughput in the power dimension should be convex in a pure NRT ad-hoc network. Accordingly, if the background noise increases in the network, this convex property is invariant. In fact, the additional interference due to the access of RT nodes is equivalent to the case when the background noise increases.

From another point of view, if we take a RT node as a special NRT node which transmits with a specified power level, the access of the special node does not affect the original projection's convex property in the other NRT power dimension. It is easy to find that the second derivative is positive when a RT node is taken as a special NRT node whose power is therefore independent of the choice of others.

Here we only show this situation for a two dimensional case in Fig. 2. When the second node is NRT, the data rate sum of R_1 and R_2 achieves maximum at one of the four points A, B, C, and D. Any projection of OD in the Q_1 dimension is convex since power of the second is flexible. Therefore, when the second user is a RT node instead, the power level on Q_2 decreases but the data rate value (H) is then on OD. The projection of HB in Q_1 dimension, EB, maintains convexity as AB does. Thus, RT node's power control result does not affect the original NRT optimal power distribution but only reduces the data rate sum. □

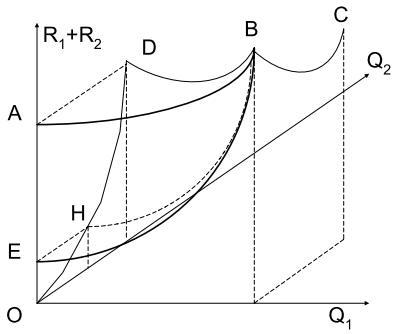

Fig. 2 Illustration for convex situation in multimedia networks

With Proposition 1, we can see that the number of NRT nodes should be limited by $2^M - 1$ where M is the number of NRT nodes (the 'all-silent' scenario is excluded). However, it is still unknown that how the scenario should be determined. Furthermore, after the NRT transmission scenario is found, the power level distribution of the RT nodes to minimize the power consumption will be needed. Therefore, we propose an optimal joint power control and scheduling process as follows.

In each time slot, given a NRT transmission scenario, the RT nodes' power distribution is examined if they can transmit under peak power after power control. That is, the RT transmission scenario is found admissible or not when the QOS is guaranteed. If it is admissible, the data rate for each NRT node under the RT power distribution and the given NRT transmission scenario is computed. In addition, the weight for each NRT node is then available according to corresponding opportunistic scheduling strategy; otherwise, the given NRT transmission scenario is neglected. After all, the NRT transmission scenarios pass the examination. The NRT nodes are scheduled to maximize the weighted rate sum and the optimization in the slot terminates. Accordingly, the flow chart of the optimal joint power control and scheduling process is shown as follows.

As can be seen from Fig. 3, the core of our optimization strategy can be divided into two parts: one is the power control for the RT nodes to minimize the interference (the sum of RT nodes' power) and the other is scheduling for the NRT nodes to meet the fairness requirements. Furthermore, according to whether there is predefined throughput share or not, the weight update for NRT case can be studied separately.

3.1 Power control for the RT nodes

Previous work in [7] illustrates that we can always find a distributed power control algorithm which converges at an exponential rate to the (optimum) minimum power vector, if one exists, in a FDMA (frequency division multiple access) or TDMA (time division multiple access) cellular system. One of the main results in [7] is a recursive algorithm in uplink distributed power control for node i in time slot L:

$$P_i(L) = \frac{\beta}{\mathrm{SINR}_i(L-1)} P_i(L-1) \tag{2}$$

where β is the predefined SINR threshold that depends on the acceptable bit error rate. That is, when the SINR requirement of each node is determined, the power distribution will be available.

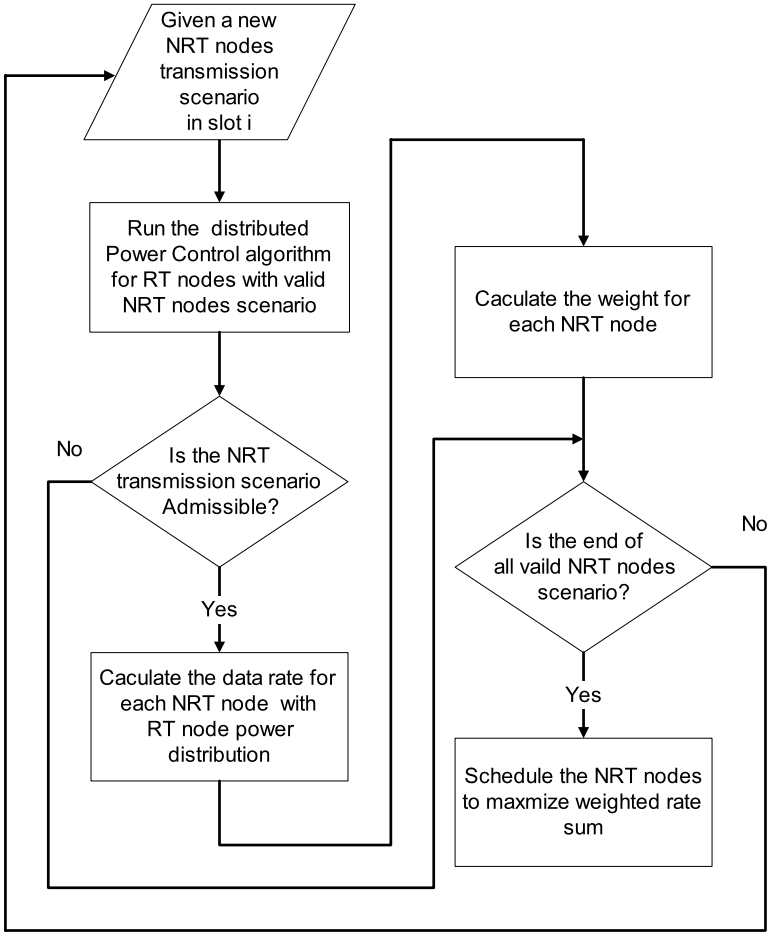

Fig. 3 Flow chart of the proposed optimization algorithm

In addition, the work in [5] shows that the optimization strategy in (2) holds in wireless ad-hoc networks under some constraints. In [5], the constraint for the power control problem in TDMA/CDMA wireless ad-hoc networks can be formulated as:

$$Z_{ij} - \frac{\beta}{G_{ij}} \sum_{k=1, k\neq i, j} Z_{kj} G_{kj} \rho_{kj} \geq \frac{\beta}{G_{ij}} \zeta \tag{3}$$

where Z_{ij} is the power level of the transmitter from node i to node j, G_{kj} is the path gain and ρ_{kj} denotes the correlation coefficient from interference source k for the correspondent receiver, node j. Moreover, ζ is the thermal noise. Generally ρ_{kj} is fixed when the system parameters are set up. That is, if the power control problem can be formulated as (3), the optimization process in (2) can be applied.

In this section, we show that this algorithm is effective for the power level distributions of the RT nodes in our UWB ad-hoc network. This proof is based on the observation to the similar problem structure in our system to that in (3).

Table 1 Parameters for RT nodes

Parameter	Description
$g_{\mathrm{RR}}(k,i)$	Path gain from RT node k to RT node i.
$g_{\mathrm{NR}}(j,i)$	Path gain from NRT node j to RT node i.
$g_{\mathrm{PR}}(p,i)$	Path gain from PNC to RT node i.
Q_j	Average power level of NRT node j in the time slot.
S_i	Average data rate of RT node i in the time slot.
P_0	Average level of pilot in the time slot.
N	Number of RT node.

Proposition 2 *For the RT nodes in the UWB multimedia ad-hoc network, the distributed power control algorithm in* (2) *converges at an exponential rate to the minimum power vector, if one exists.*

Proof The crux to prove this proposition is based on the comparison of our problem structure to the power control situation in [5]. That is, if two problems' structure is proven isomorphic, the result in (2) is also applicable to the system we consider.

As shown in Fig. 1, the interference to one node is from PNC and other nodes. According to (1), the joint optimization problem for RT nodes with a given NRT nodes transmission scenario in a given slot is formalized as follows:

$$\text{Minimize} \sum_{i=1}^{N} P_i \tag{4}$$

subject to the constraints:

$$P_i \le P_{\max} \tag{5}$$

where $P_{\max}$ is the peak power of RT node,

$$\mathrm{SINR}_i \ge \beta \tag{6}$$

and

$$\mathrm{SINR}_i = \frac{P_i g_{\mathrm{RR}}(i,i)}{S_i\left(\eta_i + T_f\sigma^2 P_0 g_{\mathrm{PR}}(p,i) + T_f\sigma^2\sum_{k=1,k\neq i}^{N} P_k g_{\mathrm{RR}}(k,i) + T_f\sigma^2\sum_{j=1}^{M} Q_j g_{\mathrm{NR}}(j,i)\right)} \tag{7}$$

where the parameters are shown in Table 1. Here (7) is the detailed representation of (1) in the piconet.

With (6) and (7), we have:

$$P_i - \frac{\beta}{g_{\mathrm{RR}}(i,i)}\sum_{k=1,k\neq i}^{N} P_k g_{\mathrm{RR}}(k,i) S_i T_f \sigma^2 \ge \frac{\beta}{g_{\mathrm{RR}}(i,i)}\left[S_i\left(\eta_i + T_f\sigma^2 P_0 g_{\mathrm{PR}}(p,i) + T_f\sigma^2\sum_{j=1}^{M} Q_j g_{\mathrm{NR}}(j,i)\right)\right]. \tag{8}$$

When a NRT transmission scenario is given, i.e., when the vector Q is available, the term in the square brackets on the right of (8) is fixed and can be seen as a background noise in the optimization. In addition, the term $S_i T_f \sigma^2$ is a constant when the UWB system parameters are fixed.

Based on the assumptions described in Sect. 2, the UWB nodes work in a half duplex mode, in accordance with the practical operating condition for TDMA/CDMA wireless ad-hoc networks. Comparing (8) and (9), it is obvious that the power control problem formulated by (4–7) has the same structure as (3) which is the power distribution problem for TDMA/CDMA wireless ad-hoc networks defined in [5]. Thus, the recursive method defined by (2) is isomorphic to our RT power control problem. □

In addition, due to the peak power constraint condition specified in (4), the original iteration algorithm could be adopted with a small modification, again similar to the work done in [5]:

$$P_i(L) = \min\left[\frac{\beta}{\mathrm{SINR}_i(L-1)} P_i(L-1),\, P_{\max}\right] \tag{9}$$

where $\min[a, b]$ returns the smaller number of a and b.

3.2 Scheduling for the NRT nodes

As stated in Sect. 1, scheduling is the process to decide which node(s) should transmit. This resource allocation decision is usually designed to maximize the throughput. In practical situations, there is a predefined fairness requirement besides the throughput demand. Accordingly, in a given time slot, the scheduling problem for NRT nodes meeting our optimization rule is formalized as follows:

$$\text{Maximize} \sum_{j=1}^{M} Y_j \tag{10}$$

subject to the constraints:

$$\prod_{j=1}^{M} Q_j \prod_{j=1}^{M} (Q_j - Q_{\max}) = 0, \tag{11}$$

$$\mathrm{SINR}_j \geq \beta \tag{12}$$

and

$$\mathrm{SINR}_j = \frac{Q_j g_{\mathrm{NN}}(j,j)}{R_j\left(\eta_j T_f \sigma^2 P_0 g_{\mathrm{PN}}(p,j) + T_f \sigma^2 \sum_{i=1}^{N} P_k g_{\mathrm{RN}}(i,j) + T_f \sigma^2 \sum_{k=1,k\neq j}^{M} Q_j g_{\mathrm{NN}}(k,j)\right)} \tag{13}$$

where the parameters are shown in Table 2.

Table 2 Parameters for NRT nodes

Parameter	Description
$g_{\mathrm{NN}}(k,i)$	Path gain from NRT node k to NRT node j.
$g_{\mathrm{RN}}(i,j)$	Path gain from RT node i to NRT node j.
$g_{\mathrm{PN}}(i)$	Path gain from PNC to RT node i.
R_j	Average data rate of NRT node j in the time slot.
M	Number of NRT node.
$Y_j = E(R_j)$	Long run expected throughput of user j.

Given NRT node j's target weight ϕ_j in the system, for any two NRT nodes j and k, the predefined fairness can be derived by using the deterministic fairness in [15]:

$$\frac{Y_j}{\phi_j} = \frac{Y_k}{\phi_k}. \tag{14}$$

With the predefined fairness, as shown in [15], the scheduling problem is equivalent to:

$$\text{Maximize} \sum_{j=1}^{M} \omega_j Y_j \tag{15}$$

subject to the constraints: (11–13) where ω_j is a non-negative constant needs to be found. That is, under the constraints (11–13), if (15) is satisfied, (10) will be solved simultaneously. Accordingly, our target is then to find the ω_j in each time slot for NRT node j.

In [15] the stochastic approximation algorithm is adopted to update the weight matrix to satisfy the deterministic fairness over multiple wireless channels. This approximation tries to find the roots of a function $f(\cdot)$ whose explicit expression is unknown. In one give time slot, the stochastic approximation reveals the root for $f(\cdot)$ at step L, which is denoted by $x(L)$, satisfies:

$$x(L) = x(L-1) - a(L-1)y(L-1) \tag{16}$$

where $a(L)$ is the step size, $y(L) = f(x(L)) + e(L)$ is the noisy measurement of $f(\cdot)$ and $e(L)$ is the observed noise. If $e(L)$ is white noise and $a(L)$ converges to zero, under certain conditions, $x(L)$ converges to the root of $f(\cdot)$. According to (10), different stochastic algorithms require different conditions. General requirements include stationarity and a certain order differential. Readers are referred to [12] for a detailed discussion. Following the results reported in [15], we consider the conditions are satisfied and the stochastic approximation can then be applied in the process of NRT nodes' power distribution.

In our case, $f(\cdot)$ is defined by $f(\vec{\omega}) = [f_1(\vec{\omega}), \ldots, f_M(\vec{\omega})]$ where:

$$f_j(\vec{\omega}) = \frac{X_j(L)}{\sum_{j=1}^{M} X_j(L)} - \frac{\phi_j}{\sum_{j=1}^{M} \phi_j} \tag{17}$$

and $\vec{\omega} = [\omega_1, \ldots, \omega_M]$ is the adaptive weight vector and $X = [X_1, \ldots, X_M]$ is the normalized rate vector in the current time slot. Using the stochastic approximation,

since the noisy observation of $f_j(\vec{\omega})$ can be found by $y_j(L)$ where:

$$y_j(L) = \frac{X_j(L)}{\sum_{j=1}^{M} X_j(L)} - \frac{\phi_j}{\sum_{j=1}^{M} \phi_j}, \tag{18}$$

the expected value of the observation error is:

$$E(e(L)) = E(y_j(L) - f_j(\vec{\omega})) = 0. \tag{19}$$

The weight matrix $\vec{\omega}$ can be found by:

$$\omega_j(L) = \omega_j(L-1) - a(L-1)y_j(L-1). \tag{20}$$

In (16), $a(L)$ should be chosen to converge to zero, following the configurations in [15], $a(L) = 1/L$ is effective. It is noticeable that our design of weight update process is different from the design in [15] where $y_j(L) = \frac{\phi_j}{\sum_{j=1}^{M} \phi_j} - \frac{X_j(L)}{\sum_{j=1}^{M} X_j(L)}$. Since ω_j is expected to denote the long term share for NRT nodes, it should decrease when the assigned resource is redundant ($y_j(L) > 0$) and increase when the resource is insufficient ($y_j(L) < 0$). The numerical results prove that (17) is more efficient than the original design in the weight convergence process.

3.3 NRT nodes transmission scenarios

As shown in Fig. 3, the determination to the NRT nodes transmission scenario is based on exhaustive search. However, if the number of users is large, such an exhaustive search may be infeasible. Thus, we use two practical methods to determine the NRT nodes transmission scenario. Both of the methods are suboptimal and are based on the previous work by Radunovic and Le Boudec [19].

The key feature of the work in [19] is an exclusive region scheduling algorithm which constructs an exclusive region surrounding the receiver. In the exclusive region, the current transmitter, as well as other transmitters outside the region, should transmit with peak power, while all the other nodes within the region should remain silent. That is, only the transmitters outside exclusive region and the corresponding transmitter of the receiver are allowed to transmit.

The optimal exclusive region radius s defined in [19] is as follows,

$$s = \left(\frac{(\delta - 2) T_f P_{\max}}{2\eta} \right)^{1/\delta}, \tag{21}$$

where δ is the reciprocal of path loss exponent, $P_{\max}$ is the maximum power of transmitter, T_f is the UWB signal frame time, and η is the homogeneous background noise power for every link. Generally, s is in the range of several meters.

In addition, in [19] the metric *proportional fairness* (PF) is formally defined as a tradeoff between system throughput and fairness:

$$\mathrm{PF} = \sum_{i=1}^{M} \log_{10}(Y_i) \tag{22}$$

where Y_i is the average throughput for link i and M is the number of links in the network. The exclusive region is proved to maximize PF in a given node distribution.

Accordingly, under the exclusive region algorithm, after the receivers are selected, the transmitter distribution can be fixed. However, the selection of the receiver is also a critical issue. Here, we consider two methods to select the receivers. One is totally randomly selection (TRS) and the other is best link first selection (BFS). For TRS, receivers are randomly selected from all links available. In this manner, the system fairness is expected to be good. For BFS, the receiver of the best link among all the links available is selected as the center of exclusive region. Therefore, the throughput is expected to be guaranteed. Finally, the integrated effect of each sub-optimal selection methods can be compared in terms of PF.

4 Simulation results

4.1 Performance metrics

Besides the proportional fairness, three long-term metrics are considered in our simulations: RT power (P), NRT throughput (Y), and fairness index (F). For the RT nodes, we study how the power of the RT node varies in the iteration process. In addition, the power distribution result after iteration is calculated. For the NRT nodes, we assume that each transmitter generates packets according to a Poisson distribution with aggregate rate λ packets/ms and the inter-arrival time is denoted by $1/\lambda$. The NRT throughput is defined as the average data rate over the simulation period. In the predefined fairness case, fairness index can be denoted by:

$$F = \frac{\left[\sum_{m=1}^{M}(Y_m/\phi_m)\right]^2}{M\sum_{m=1}^{M}(Y_m/\phi_m)^2} \tag{23}$$

where ϕ_m is the corresponding share for NRT node m.

4.2 Simulation parameters

For TH-PPM modulations, T_f is fixed at 10 nanoseconds in our simulation. Thus, the maximum data rate constraint is $R_{\max} = 1/T_f = 100$ Mbps. In all scenarios, the data rate of RT node is fixed at $S = 1$ Mbps. Other system parameters are based on those reported in [4]. Specifically, the background noise power is assumed the same for every node as $\eta = 2.568 \times 10^{-21}$ $\mathrm{V}^2\mathrm{s}$. The ratio between the peak power and the background noise power is set to be 5.136×10^{-9} and, therefore, the exclusive region radius given by (21) is about 5 meters. The interference parameter between UWB impulses is $\sigma^2 = 1.9966 \times 10^{20}$. Since most interference of the pilot is caused by PNC and PNC is required to be heard by every node, we assume that the pilot interference equals the effect when PNC always transmits with peak power. A required SINR at the receiver end is fixed at 30 (14.7 dB).

The UWB propagation model is described by path loss, shadowing and multipath, and is given by:

$$g(m,n) = r_{m,n}^{-\delta} \cdot 10^{\upsilon_{m,n}/10}\zeta_{m,n}. \tag{24}$$

Table 3 Simulation parameters

Parameter	Value
Rate and Power adaptation period T (ms)	2
Path loss exponent, δ	4.0
Deviation of shadow fading σ_s (dB)	8.0
RT data rate S (Mbps)	1
NRT data rate max $R_{\max}$ (Mbps)	100
RT peak power $P_{\max}$	5.136×10^{-9}
Pilot power P_0	5.136×10^{-9}
UWB multipath channel model	CM2
No. of multipath N_R	10
Multiaccess interference parameter σ^2	0.002
Background noise for RT and NRT η	2.568×10^{-21}
Required SINR at receiver end β	30
Initial value of iteration for weight matrix ω	2

Specifically, $r_{m,n}$ is the distance between node m and node n, δ is the path loss decay factor, and the shadowing factor $\upsilon_{m,n}$ is a Gaussian random variable with mean zero and deviation σ_s. In addition, to describe multipath effect, the modified Saleh–Valenzuel (S–V) model, defined by 802.15.3a standard [6], is adopted. The multipath signal is modeled by asynchronously arriving clusters containing many asynchronous rays. The channel coefficient for the kth ray in the lth cluster $\alpha_{m,n,k,l}$ is found to closely follow the log-normal distribution. Thus, with $\zeta_{m,n} = \sum_{l=1}^{L} \sum_{k=1}^{K} \alpha_{m,n,k,l}^2$, expression (22) can be derived. In [6] four sets of parameters have been found to present the key property of observed UWB multipath channels. The second set of parameters (CM2), based on NLOS (0–4 m) channel measurements, is used in our simulations since it is a tradeoff between LOS (0–4 m) and LOS (4–10 m).

Statistics in [22] suggests that the number of nodes should be less than 10 in a high data rate (over 10 Mbps) PPM UWB system. Thus, we assume that total number of nodes is around 10 and the transmitter number $(N + M)$ is around 5. Specifically, $N = 2$ is used as a default. All the nodes are distributed uniformly and randomly in an area of 11 m $\times$ 11 m, the size of a typical home or small office. To study the scheduling performance in the predefined fairness scenario, we assume that all nodes share the slots equally. For instance, for $M = 4$, $\phi = (0.25, 0.25, 0.25, 0.25)$ is set.

The rate and power adaptation period is set $T = 2$ ms. The path loss and the shadowing are assumed constant in each adaptation period and the multipath fading is averaged over n_s times (n_s is assumed to be four in our calculation). In addition, the RT and NRT nodes are assumed to distribute uniformly in the area at the beginning of simulation. In every simulation, 1,000 frames are generated, i.e., the simulation time is 2 s.

Some key simulation parameters are listed in Table 3 for easy reference.

Two traffic models are used to evaluate NRT throughput. One is the bulk traffic model used in [9], the other is a modified downlink model given by [1]. For traffic model 1, packets are assumed arriving consecutively in each slot. For traffic model 2, a sequence of bursts is used. Each burst is a sequence L1, L2, L3, L1 with interval T1. Here L1 models the SYN and the minimum packet length, L2 resembles the TCP slow

Table 4 Parameters of traffic model 2

Short packet L1	80 bytes
TCP slow start L2	1,500 bytes
Data trunk size L3	Equally selected between 6500 bytes and 625000 bytes
Round trip delay T1	0.3 s
Burst interval T2	Exponential distribution with mean 10 s
Single packet size	1500 bytes

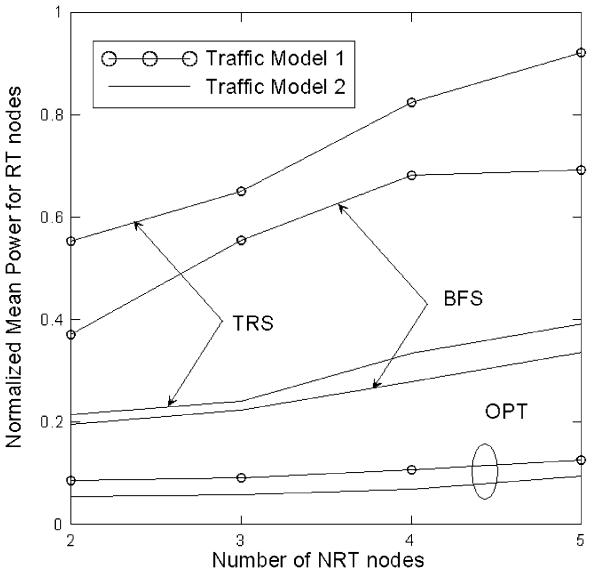

Fig. 4 Impact of number of NRT nodes on the normalized RT node power level

start, L3 denotes the data chunk size and T1 is the round trip time. In addition, T4 is set between each burst. The parameters used in the traffic model are given in Table 4.

4.3 Results and discussions

In this section, we report the main results derived from the joint optimization in the exhaustive search optimal method (called OPT). In addition, we also compare some joint optimization performance to that under TRS and BFS strategies.

First, Fig. 4 shows the long-term power variation results under various number of NRT nodes. We can see that when then number of NRT nodes is larger, the RT power consumptions under all configurations rises due to the increasing NRT interference. Since traffic model 1 has a heavier load than traffic model 2, the specific RT power level is higher under the former traffic pattern for OPT, BFS, and TRS. In addition, for both of the traffic models, OPT achieves the smallest power level since it explores the full NRT distribution space. The plausible argument for explaining why BFS consumes less power than TRS is as follows. BFS always selects the best NRT transmission link which generally has a small transmission range, the transmitter then, with a high probability, situates in the receiver's exclusive region than the TRS cases. Since no other transmitters can transmit in the exclusive region, the high

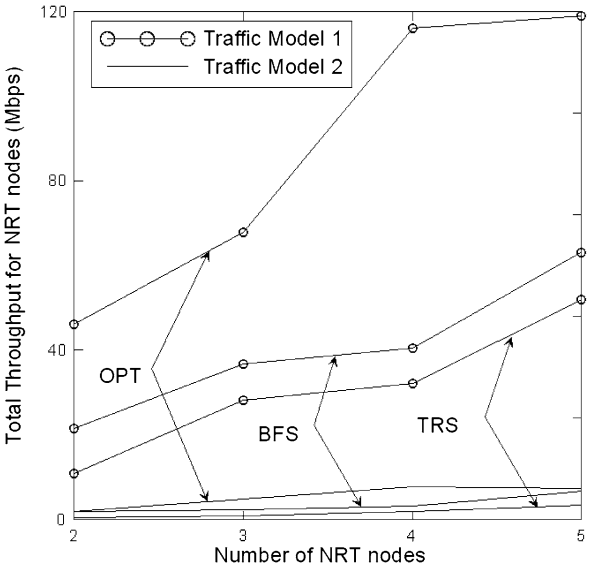

Fig. 5 Impact of number of NRT nodes on the total throughput of NRT nodes

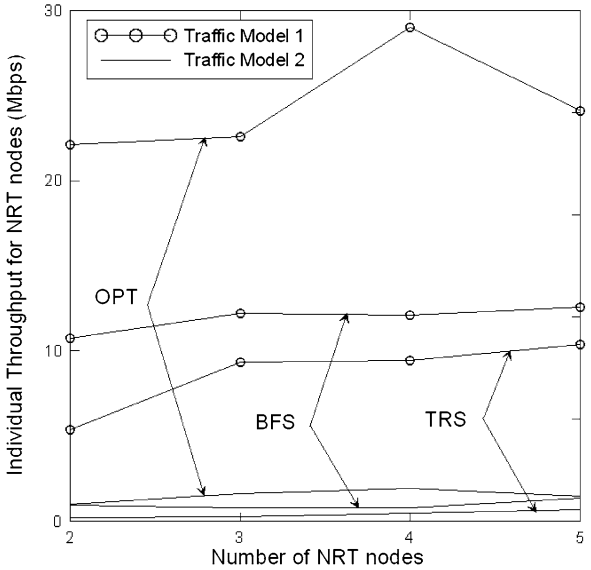

Fig. 6 Impact of number of NRT nodes on the average throughput of NRT nodes

interference caused by the close transmitters is reduced, and therefore, the long term effect of the link's transmitter to the other transmitters is much less.

Secondly, the total throughput and individual throughput of NRT nodes are shown in Figs. 5 and 6. We can see that OPT achieves the best performance, while BFS outperforms TRS under both traffic models. From Fig. 5, under all configurations, system throughput sum rises when the NRT node number increases. By contrast, in Fig. 6, individual throughput for OPT case is observed convex due to the increasing interference. Since the total throughput is increasing, we can conclude that the scenario of $(N, M) = (2, 5)$ is still feasible.

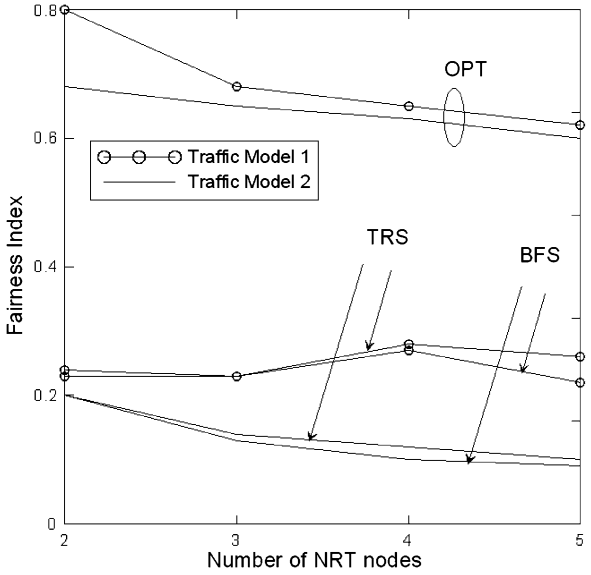

Fig. 7 Impact of number of NRT nodes on fairness index

Table 5 Impact of NRT power level distribution determination on algorithm running times (unit: minute)

Number of NRT	OPT	TRS	BFS
2	12.1	1.7	1.7
3	27.6	2.7	2.8
4	44.9	3.8	3.8
5	58.4	5.3	5.3

Thirdly, the fairness index and proportional fairness index are compared in Figs. 7 and 8. OPT still has the best fairness and proportional fairness. And TRS has a slightly better fairness index than BFS but a worse proportional fairness index. In addition, we can see that BFS approaches OPT closely in PF, especially under a practical situation (i.e., traffic model 2). Since PF is considered a good trade off between throughput and fairness, we can conclude that BFS is a good substitute for OPT when the optimal exhaustive search is infeasible.

Finally, the impact of NRT power level distribution determination methods to simulation time is shown in Table 5. All the results are the average values over the total simulation time. As can be seen, OPT is the most time consuming among the three methods. TRS and BFS have almost the same running time since both of them have to deal with a similar exclusive region finding process.

In summary, when the system is sensitive to performance (especially RT power consumption) and system scale is small, OPT could be used; otherwise, BFS could be used as a good substitute.

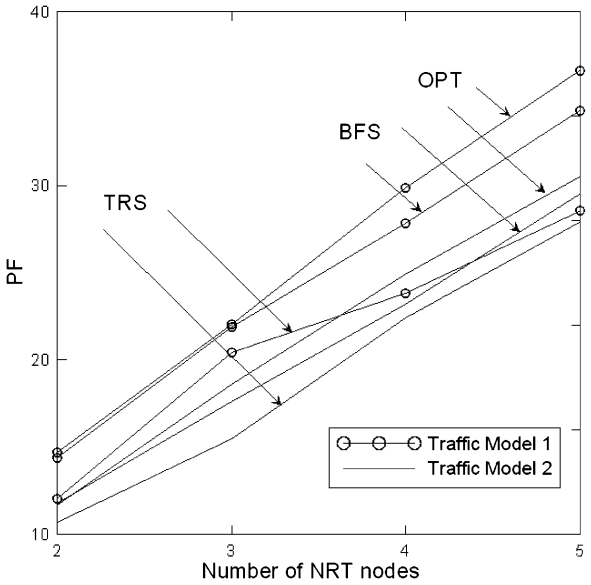

Fig. 8 Impact of number of NRT nodes on PF

5 Conclusions

We have presented a joint power and rate optimization method for UWB ad-hoc multimedia networks. The proposed strategy can maximize system throughput while meeting the fairness requirement for NRT nodes and minimizing the power level of RT nodes. Simultaneously, the required SINR for both applications are guaranteed.

Since the optimal strategy is based on the exhaustive search in the NRT node distribution space, for the case where system scale is large, two sub-optimal strategies characterized by 'totally randomly selected' and 'best link first selected' are consequently compared. The former strategy intends to achieve a good fairness between users while the latter one performs better in the RT power consumption, the NRT throughput and the proportional fairness than the former one. Therefore, the latter strategy may be a good substitute when the optimal strategy is infeasible. Furthermore, if the network scale increases to tens of nodes, the single piconet structure may not be appropriate any more for an efficient radio resource allocation process. Consequently, a practical approach would be used to perform the resource allocation process under a hierarchical network structure [3].

In our analysis, we have treated the real-time application as a constant bit rate source. However, the RT applications such as broadcast videos are generally modeled as variable bit rate (VBR) sources. If this model is introduced into our optimization, we have to take the maximum data rate as the rate of RT nodes because there is no chance for the device to respond to its rate to the PNC. This measurement definitely wastes some radio power. However, how to optimize the VBR RT application's power level may be connected with a different design. Future work thus could be done in the optimization strategy in a different design to UWB ad-hoc multimedia networks, according to the requirement from a different environment. Apart from the fact that the VBR RT case could be taken into consideration, the scheduling could also be more complicated if the content length of NRT applications changes greatly.

Acknowledgements The authors would like to thank the anonymous reviewers for their insightful and constructive comments that have greatly improved this paper.

References

1. Anderlind E, Zander J (1997) A traffic model for non-real-time data users in a wireless radio network. IEEE Commun Lett 1(2):37–39
2. Borst S, Whiting P (2001) Dynamic rate control algorithms for HDR throughput optimization. In: Proc IEEE INFOCOM '01, Anchorage, Alaska, April 2001
3. Cruz RL, Santhanam AV (2003) Optimal routing, link scheduling and power control in multi-hop wireless networks. In: Proc IEEE INFOCOM2003, pp 702–711
4. Cuomo F, Martello C, Baiocchi A, Capriotti F (2002) Radio resource sharing for ad-hoc networking with UWB. IEEE J Sel Areas Commun 20(9):1722–1732
5. Elbatt T, Ephremides A (2004) Joint scheduling and power control for wireless ad hoc networks. IEEE Trans Commun 3(1):74–85
6. Foerster J (2003) Channel modeling sub-committee report final. IEEE P802.15-02/490r1-SG3a
7. Foschini G, Miljanic Z (1993) A simple distributed autonomous power control algorithm and its convergence. IEEE Trans Veh Technol 42(4):641–646
8. Helal D, Rouzet P (2003) ST microelectronics proposal for IEEE 802.15.3a Alt PHY. IEEE P802.15-02/372r8
9. Hossain E, Kim DI, Bhargava VK (2004) Analysis of TCP performance under joint rate and power adaptation in cellular WCDMA networks. IEEE Trans Wirel Commun 3(3):865–879
10. http://www.UWB.org
11. Kelly F (1997) Charging and rate control for elastic traffic. Eur Trans Telecommun 9:33–37
12. Kushner H, Clark D (1978) Stochastic approximation methods for constrained and unconstrained systems. Springer, Berlin
13. Legrand F et al (2003) U.C.A.N.'s ultra wide band system: MAC and routing protocols. In: Proc IWUWBS2003
14. Liu X, Chong E, Shroff N (2001) Transmission scheduling for efficient wireless network utilization. In: Proc IEEE INFOCOM2001, pp 776–785
15. Liu Y, Knightly E (2003) Opportunistic fair scheduling over multiple wireless channels. In: Proc IEEE INFOCOM2003, vol 2, pp 1106–1115
16. Liu Y, Knightly E (2003) WCFQ: an opportunistic wireless scheduler with statistical fairness bounds. IEEE Trans Wirel Commun 2(5):1017–1028
17. Negi R, Rajeswaran A (2004) Scheduling and power adaptation for networks in the ultra wide band regime. In: Proc IEEE GLOBECOM2004, vol 1, pp 139–145
18. Ofuji Y, Abeta S, Sawahashi M (2003) Fast packet scheduling algorithm based on instantaneous SIR with constraint condition assuring minimum throughput in forward link. In: Proc IEEE WCNC2003, vol 2, pp 860–865
19. Radunovic B, Le Boudec J-Y (2004) Optimal power control, scheduling, and routing in UWB networks. IEEE J Sel Areas Commun 22(7):1252–1270
20. Toumpis S, Goldsmith AJ (2003) Capacity region for wireless ad-hoc networks. IEEE Trans Wirel Commun 2(4):736–748
21. Win MZ, Scholtz RA (1998) On the robustness of ultra-wide bandwidth signals in dense multipath environments. IEEE Commun Lett 2(2):51–53
22. Win MZ, Scholtz RA (2000) Ultra-wide bandwidth time-hopping spread-spectrum impulse radio for wireless multiple-access communications. IEEE Trans Commun 48(4):679–689

Yang Liu got his B.Eng. and M.S. degrees from the Southeast University, Nanjing, PR China in 1997 and 2001, respectively. He got his Ph.D. degree in Electrical and Electronic Engineering from the University of Hong Kong in 2006. His research interestes are ad hoc networking, 4G wireless communications, and UWB networks. He is now a Design Engineer in Huawei Technologies in Shenzhen, PR China.

Yu-Kwong Kwok is an Associate Professor in the Department of Electrical and Electronic Engineering at the University of Hong Kong (HKU). Before joining the HKU in August 1998, he was a visiting scholar for one year in the parallel processing laboratory at the School of Electrical and Computer Engineering at Purdue University. He recently served as a visiting associate professor at the Department of Electrical Engineering-Systems at University of Southern California from August 2004 to July 2005, on his sabbatical leave from HKU.
He received his B.Sc. degree in Computer Engineering from the University of Hong Kong in 1991, the M.Phil. and Ph.D. degrees in Computer Science from the Hong Kong University of Science and Technology (HKUST) in 1994 and 1997, respectively. His research interests include distributed computing systems, wireless networking, and mobile computing. He is a Senior Member of the IEEE. He is also a member of the ACM, the IEEE Computer Society, and the IEEE Communications Society. He received the Outstanding Young Researcher Award from HKU in November 2004.

J. Wang is currently a Professor and a Chair in the Department of Electronics, the University of Kent. His research interests are in the areas of CDMA, OFDM, MIMO, channel coding, scheduling for wireless communications. He was a Technical Chairman of IEEE Workshop in 3G Mobile Communications in 12/2000. Professor Wang has published over 100 papers, including more than 30 IEEE Transactions/Journal papers. He has written/edited two books, entitled "Broadband Wireless Communications" (Kluwer, Boston, MA, 6/2001) and "Advances in 3G Enhanced Technologies for Wireless Communications" (Artech House, Norwood, MA, 2/2002), respectively.